Journal of Physics: Conference Series

PAPER • OPEN ACCESS

Numerical study of airfoil used for helicopter rotor tip to investigate the enhancement in the aerodynamic characteristics using active flow control at forward flight conditions

To cite this article: T M Tawfik and M M Abdelrahman 2023 *J. Phys.: Conf. Ser.* **2616** 012004

View the article online for updates and enhancements.

You may also like

- Numerical and experimental analysis on the helicopter rotor dynamic load controlled by the actively trailing edge flap
Z X Zhou, X C Huang, J J Tian et al.
- Fibre-optic measurement of strain and shape on a helicopter rotor blade during a ground run: 1. Measurement of strain
Stephen W James, Thomas Kissinger, Simone Weber et al.
- Exploring Martian Magnetic Fields with a Helicopter
Anna Mittelholz, Lindsey Heagy, Catherine L. Johnson et al.

This content was downloaded from IP address 195.43.0.86 on 12/03/2024 at 07:18

Numerical study of airfoil used for helicopter rotor tip to investigate the enhancement in the aerodynamic characteristics using active flow control at forward flight conditions

T M Tawfik[1,2], M M Abdelrahman[3]

[1]Graduate PhD research student, Aerospace Engineering Department, Cairo University
[2]Helicopter technical support and maintenance engineer at Petroleum Air Services
[3]Professor of Aerodynamics, Aerospace Engineering Department, Cairo University

tarek.mokhtar24@gmail.com.

Abstract. Helicopter forward flight is the most important state of flight due to time spent in this mode during the complete helicopter trip. In this study, a main rotor blade tip airfoil was simulated to obtain the effect of applying active flow control on the tip part of the rotor blade. A blowing excitation jet is applied to the leading edge of the airfoil just before the separation point with small momentum and high frequency to enhance the near wall boundary layer characteristic. This jet is used with different amplitude, frequency and excitation location from a leading edge to study the effect of this parameter. A numerical model is used to solve two different angles of attack and all results are compared with NACA report that used the same helicopter hub and airfoil. Results show good agreement with the experimental results and the chosen excitation parameter gives good enhancement to the performance of the airfoil used in the tip part of the helicopter blade in this mode of flight. Performance represented in lift and drag and lift to drag ratio shows improvement, reaching about 10% increase in lift and 30% decrease in drag, which means more than 50% change in lift to drag ratio. Furthermore, this study gives a good estimation of the best excitation location that is required for real application on the helicopter blade to improve of forward flight performance.

1.Introduction

In the commercial helicopter, the daily routine flight is divided into four states of flight, starting from hover, passing through climb, forward flight, descent and hover again. Climb and descent state of flight are a transient state of flight and performance of these two states of flight is not more important than the other states of flight. Hover and forward flight are the most important states of flight because of the time that the helicopter spends in these modes. A helicopter in hovering flight maintains a constant position over a predetermined point, usually a few feet above the ground. To hover, the lift and thrust produced by the rotor system must act straight up and equal the weight and drag that act straight down. You can adjust the amount of main rotor thrust while hovering to maintain the desired hovering altitude. This is accomplished by varying power and changing the angle of attack of the main rotor blades as needed. Thrust acts in the same vertical direction as lift in this case. The tip-path plane is tilted forward during forward flight, tilting the total lift-thrust force forward from vertical. As shown in Figure 1, the resultant lift-thrust force can be divided into two components: lift acting vertically upward and thrust acting horizontally in the direction of flight. Aside from lift and thrust, there is also weight (the downward acting force) and drag (the rearward acting or retarding force of inertia and wind resistance). As the helicopter moves forward, it loses altitude due to the lift lost as thrust is diverted forward. As the helicopter accelerates, the rotor system becomes more efficient due to increased airflow. As a result, there is excess power over what is required to hover. With continued acceleration, airflow through the rotor disc increases even more, resulting in even more excess power.

Content from this work may be used under the terms of the Creative Commons Attribution 3.0 licence. Any further distribution of this work must maintain attribution to the author(s) and the title of the work, journal citation and DOI.
Published under licence by IOP Publishing Ltd

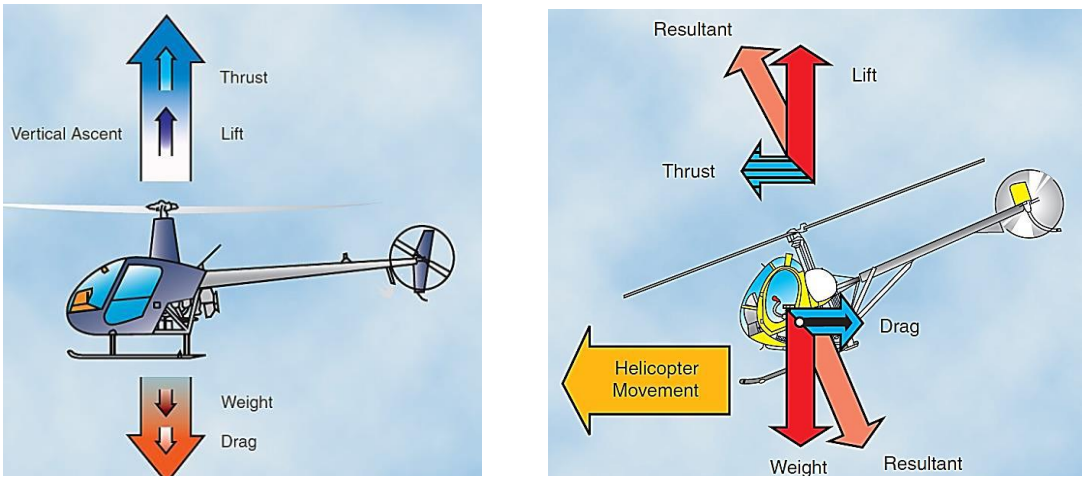

Figure 1. Helicopter forces during hover(left) and forward flight (right) [Rotorcraft Flying Handbook (FAA-H-8083-21)].

In forward flight, as the helicopter accelerates, induced flow drops to near zero at the forward disc area and increases at the aft disc area. This causes the rotor blade to flap up at the front disc area and down at the back disc area. Maximum displacement occurs 90° in the direction of rotation because the rotor acts like a gyro. As a result, the helicopter has a tendency to roll slightly to the right as it accelerates. This effect is reduced by dynamically changing the angle of attachment of the blade during its rotation, which increases at the retreating side to provide more lift. This situation of a high angle of attach and less relative velocity on the retreating blade increases separation and leads to lift dissymmetry; however, as shown in Figure 2, the right half of the rotor disc is travelling faster than the left half. The advanced half of the disc is referred to as the advanced side, and the retreating half is referred to as the retreating side. The velocity of the lift on the retreating half of the disc will be lower than the velocity of the lift on the advancing half of the disc. In this study, the use of active flow control will assist this blade in delaying separation and gaining more lift, thereby improving the overall performance of the blade and hub system.

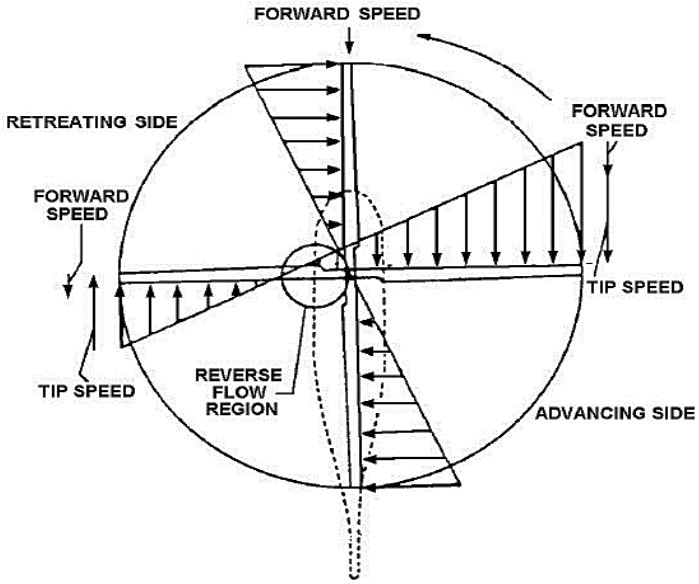

Figure 2. Velocity distribution in forward flight [1].

2. Literature Review

Active flow control is widely used in aviation applications and it represents the new way to enhance the flow in the boundary layer. The impact of trailing edge flaps on retreating blade side stall was investigated by Fotios K. Tsiachris [19]. He studied numerical simulations of a NACA 0015 airfoil with a plain flap at trailing edge. These simulations performed for 2D incompressible flows over an airfoil with an oscillating pitch at its quarter chord axis. The study discovered that for the decreased frequency range of 0.128 to 0.180, a flap size with a nominal chordal length of C_l = 15% of C was successful in reducing sectional pitching moment undershoot. At Politecnico di Milano [20], a new experimental-numerical work on dynamic stall control for helicopter performance enhancement has begun. The focus of this research is on experimental action on oscillating airfoils. As a result, a blade section model with a NACA23015 airfoil was created and tested to compute the performance of activated flaps on a thicker airfoil subjected to a trailing edge stall process. The results of the testing on the NACA23015 airfoil show a considerable effect in terms of control, with stall delayed. Patrick Bowles et al. [21] used a flow sensor to detect separation. On the upper wing surface, a small fixed high-bandwidth pressure sensor has been added near the leading-edge chord. Unstable plasma actuator is applied to the forefront of the wing to control the gas flow. The actuator is connected to the direction of the span to effectively mix the external volume of the border layer with a low volume near the wall of the air pressure surface, causing delay in separation. Leading edge slats (LES) and the hovering capability of the UH-60A helicopter rotors were both studied by Yashwanth Ram Ganti [22]. Simulations were done on a He UH-60A helicopter blade with two different slat configurations and 40% span slats. According to the enhanced mesh, the slatted rotors performance output compared favorably to the original UH-60A helicopter rotors with larger collective angles while only experiencing a little performance hit at a moderate collective angle setting. An "Active Gurney Flap" is a small, flat tab installed on the pressure side of a rotor blade at its TE that frequently deploys and retracts throughout the rotation cycles of the main hub blade. In order to preserve current flying performance capabilities while considerably reducing power consumption or main rotor tip speed, the Active Gurney Flap looks to be a potential option, especially in the case of retreating blade stall. The flap is activated by the helicopter's blades, and it can help to prevent the helicopter from hitting obstacles or losing altitude. Wienczyslaw and Sznajder [23] developed an approach for modelling active flow control devices, such as the Active Gurney Flap, which used to enhance the performance and environmental impact of helicopters. This innovative technology will allow less power consumption or lower main rotor tip speeds, while still maintaining current flight performance. It seems like a wise decision, given the current state of the helicopter industry.

3.Helicopter Dynamic Stall

At high forward flying speeds, especially after attaining VNE (velocity never exceed) or during manoeuvres with high load factors, dynamic stall starts on the rotor blades during retreating travel, resulting in the following opposing impacts on helicopter total performance:

- A control system increased loads and difficulties.
- The helicopter is vibrating a lot and it's not doing well in terms of velocity, lift, and the ability to manoeuvre.
- Aerodynamic limitations for example, loss of control.
- Occurrence of an aeroelastic unsteadiness called flutter stall, causing damage and extreme vibration to blade structural and cabin.

The dynamic stall phenomenon can have a significant impact on helicopter performance and flight dynamics, and it is a common issue in rotorcraft research. When the rotational and forward speeds of a helicopter combine to create large changes in local velocities over the rotor blades, dynamic stall can occur. This can cause a number of negative effects on the helicopter, including decreased lift and increased drag. Consequently, it is important to understand the phenomenon and take appropriate measures to prevent it from happening, as seen in Figure 3. The fundamental consequence of the speed structure is an increase in velocity at local points on the travelling blade and a drop on the retreating blade; as a result of these changes in speed, the rotor becomes unbalanced or out of trim. Rotor trimming

is accomplished through the use of cyclic input pitch, in which the rotor blade moves up when the local velocity is low and down when the local velocity is high. Then, as the retreating blade meets a quick shift of angle of attack due to the mixture of a pitching and plunging action, flow separation and stall occur on a rotor in a very dynamic and time-dependent manner. As a result, the stall and flow separation growth on the blade in retreating side differ from the stall mechanism displayed by the same airfoil under static conditions, as stated in the next paragraph.

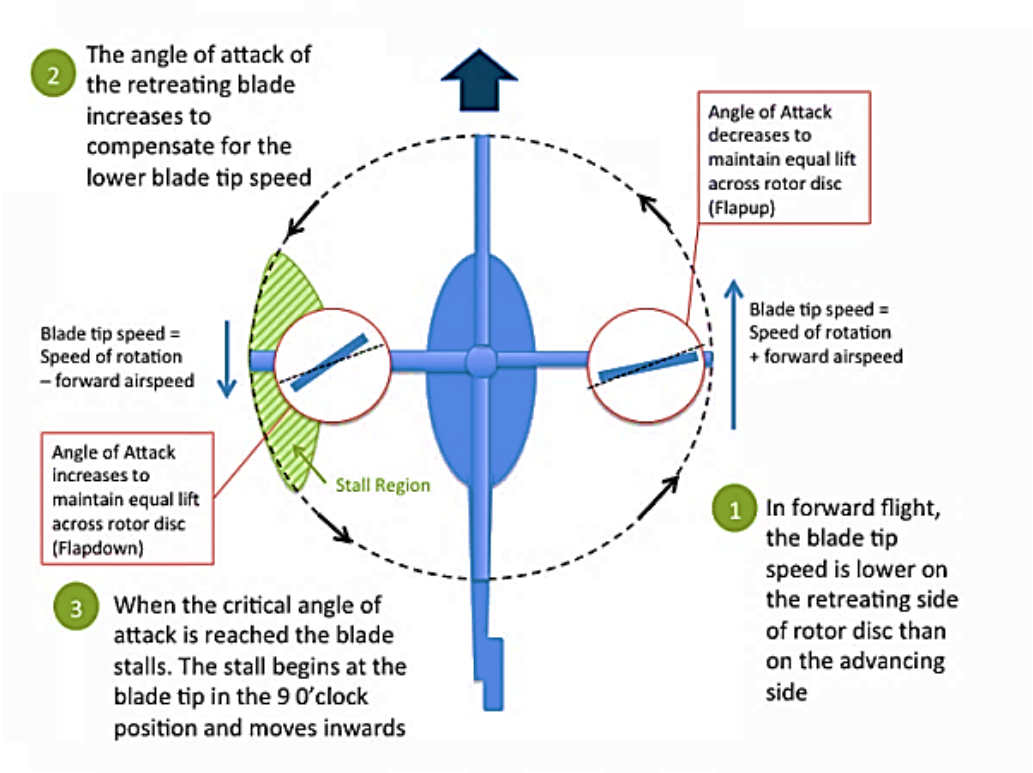

Figure 3. Stall region [skybrary aviation safety].

4.Governing equation

There are two essentially distinct techniques to deducing the equations that describe fluid motion: the "Eulerian" explanation and the "Lagrangian" explanation. The two points of view are named after the Swiss mathematician "Leonhard Euler," who lived from 1707 to 1783, and "Joseph-Louis Lagrange," who lived from 1736 to 1813.

- Eulerian explanation

A fluid is moving relatively in a fixed reference frame. Time and geographical location are employed as independent variables in this reference frame as (t, r). The fluid components that determine the physical condition of the fluid flow, such as mass, density, pressure, and flow velocity, are regarded as dependent variables since they are functions of the other independent variables. Their derivatives' ensuing partial representation with regard to (t, r). As an illustration, the flow velocity at each place and time is provided by: u (r, t), but the comparable acceleration at any position and time is supplied by: u (r, t):

$$a = \frac{\partial u(t,r)}{\partial t}_{r=constant} \tag{1}$$

- Lagrangian explanation

The Lagrangian explanation describes the fluid in terms of its basic fluid components. The "names" of various fluid components differ, for example, their spatial coordinates at any given fixed time t, which is taken to be q. The particle location r (t, q) is sometimes referred to as a dependent variable. The independent variables are (t, q). The rate of change with respect to time in a reference frame flowing with the fluid element may then be questioned; the answer will depend on the time and particle name. As an illustration, the acceleration will be as follows if a fluid element has some velocity termed u as a function of (t, q):

$$a = \frac{\partial u(t,q)}{\partial t}_{q=constant} \tag{2}$$

In conclusion Newtonian fluid motion is described by the equations expressed in:

Continuity will be in the form:

$$\frac{\partial \rho}{\partial t} + u_k \frac{\partial \rho}{\partial x_k} + \rho \frac{\partial u_k}{\partial x_k} = 0 \tag{3}$$

Energy will be summarized as:

$$\rho \frac{\partial e}{\partial t} + \rho u_k \frac{\partial e}{\partial x_k} = -p \frac{\partial u_k}{\partial x_k} + \frac{\partial}{\partial x_j}\left(k \frac{\partial T}{\partial x_j} \right) + \lambda \left(\frac{\partial u_k}{\partial x_k} \right)^2 + \mu \left(\frac{\partial u_j}{\partial x_i} + \frac{\partial u_i}{\partial x_j} \right) \frac{\partial u_j}{\partial x_j} \tag{4}$$

Navier-Stokes will be the equations:

$$\rho \frac{\partial u_j}{\partial t} + \rho u_k \frac{\partial u_j}{\partial x_k} = -\frac{\partial p}{\partial x_j} + \frac{\partial}{\partial x_j}\left(\lambda \frac{\partial u_k}{\partial x_k} \right) + \frac{\partial}{\partial x_i}\left[\mu \left(\frac{\partial u_i}{\partial x_j} + \frac{\partial u_j}{\partial x_i} \right) \right] + \rho f \tag{5}$$

Last Equation is state equation:

$$p = p(\rho, T) \tag{6}$$

And caloric equation:

$$e = e(\rho, T) \tag{7}$$

The continuity, energy, and state equations each provide a separate scalar equation, but the Navier-Stokes equation combines three scalar equations into a single vector equation. The components of pressure (p), velocity (uj), density (ρ), temperature (T), and internal energy (e) make up the seven unknowns. From past experimental findings, it is expected that the parameters λ, μ and k, which may be constants or specified functions for temperature and pressure, will be known.

5.Numerical Method

The mechanics of any fluid movement around or inside of a person are governed by three basic rules. According to Newton's second law, mass, energy, and fluid acceleration are all conserved. There are now five governing differential equations since Newton's second law is written as a vector with three directions. These equations, often referred to as "Navier-Stokes equations," were created at the start of the nineteenth century to create the fundamental equation regulating flow. The simulation process flow chart shown in Figure 4 shows that although certain appealing solutions to these equations have been known for a while, their application to real-world flow problems can only be achieved via numerical solutions. Several CFD (computational fluid dynamics) algorithms were introduced to calculate air loads and flow over helicopter blades, heads, and bodies, as well as to investigate the flow over rotors. Modern CFD techniques became aware of these new methodologies during the last century. Chang [3] updated the flow solver "FLO22" to simulate helicopter rotors, while Caradonna [2] updated the transonic disturbance concept to lifting rotors. The turbulent flow over the four-bladed rotor robin helicopter was simulated using the NASA "Glenn Research Center" WIND code [4]. Given the flexibility of CFD analysis today, practically any type of vehicle, including rotorcraft and fixed-wing aircraft, may have its flow studied. Long before computers were able to quickly and efficiently complete an enormous number of complex calculations, aeronautical engineers used three major research methodologies to show the flow field over an aircraft. Early rotor modelling techniques were based on Prandtl's wing lifting line theory. Individual blades were represented as lines of vortices in these methods, and a wake was represented as a twisted helix. Flight testing is very time- and money-consuming, and the answers that are found are usually changed from the ideal parameters that were first found.

Despite the fact that the wind tunnel approach is more effective for solving common issues such as predicting fuselage drag reduction. As a result, the helicopter industry is quickly incorporating CFD methodologies into its design process in order to reduce the number of wind tunnel tests and enhance the number of configurations that are numerically assessed. The modelling of this case study and the discussion of this tactic will be handled in the next section.

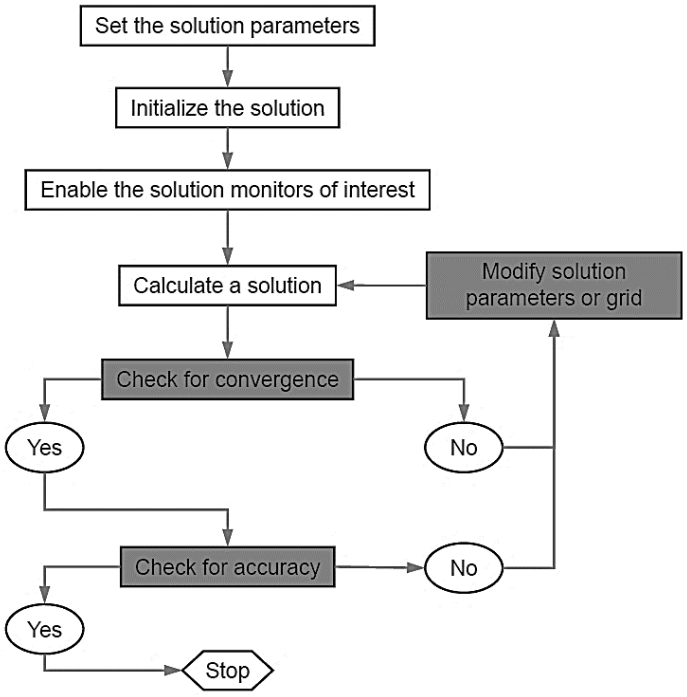

Figure 4. Flow chart of CFD process.

6.Model and analysis methods

A 2-D airfoil (at blade at tip) aerodynamics is investigated in the forward flight condition with domain geometry as in Figure 5 and validated against available data from wind tunnel published measurements for different angles of attack in the benchmark case without control. Baseline case results are the comparative of the controlled cases.

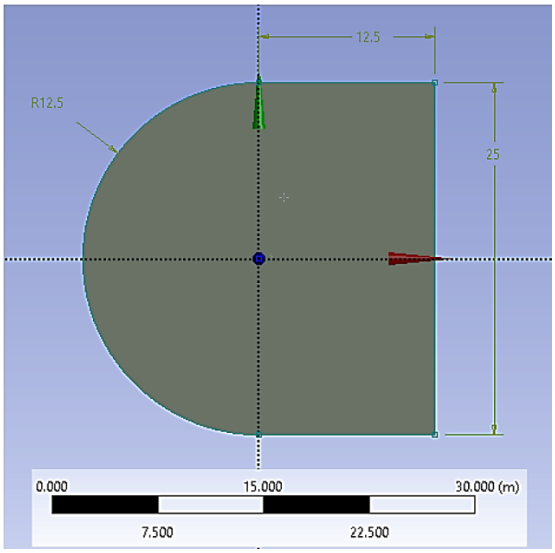

Figure 5. domain geometry.

6.1. Benchmark Case

In the benchmark case, the tip airfoil "NACA RC(6)-08" geometry in the selected hub assembly [5] is modeled as in Figure 6. Three major reasons drive the design of a specific airfoil to function at the rotor tip; For the airfoil to maintain lift when the rotor blade is on its travel when rotor is at disc's retreating side, it must have high lift coefficients at the maximum available in the Mach number value of 0.35-0.50. The airfoil also should have drag-divergence for Mach number at high value where c_l is low in order to minimize the amount of rotor power needed while the rotor blade is moving in direction along rotor disc. To prevent the rotor blade from twisting in torsional direction and to control its loads, the airfoil pitching moment must be kept as low as possible for each condition coming across the disc, but mainly for $M \approx 0.80$. The baseline tip section of the blade was the RC(6)-08 since it has demonstrated characteristic [6] in the tip part of the blade. The pitching-moment of the RC(6)-08 airfoil is very low throughout a wide range of M and, the maximum lift coefficients are extremely high at M up to 0.5, and the drag divergence M is extremely high at low α.

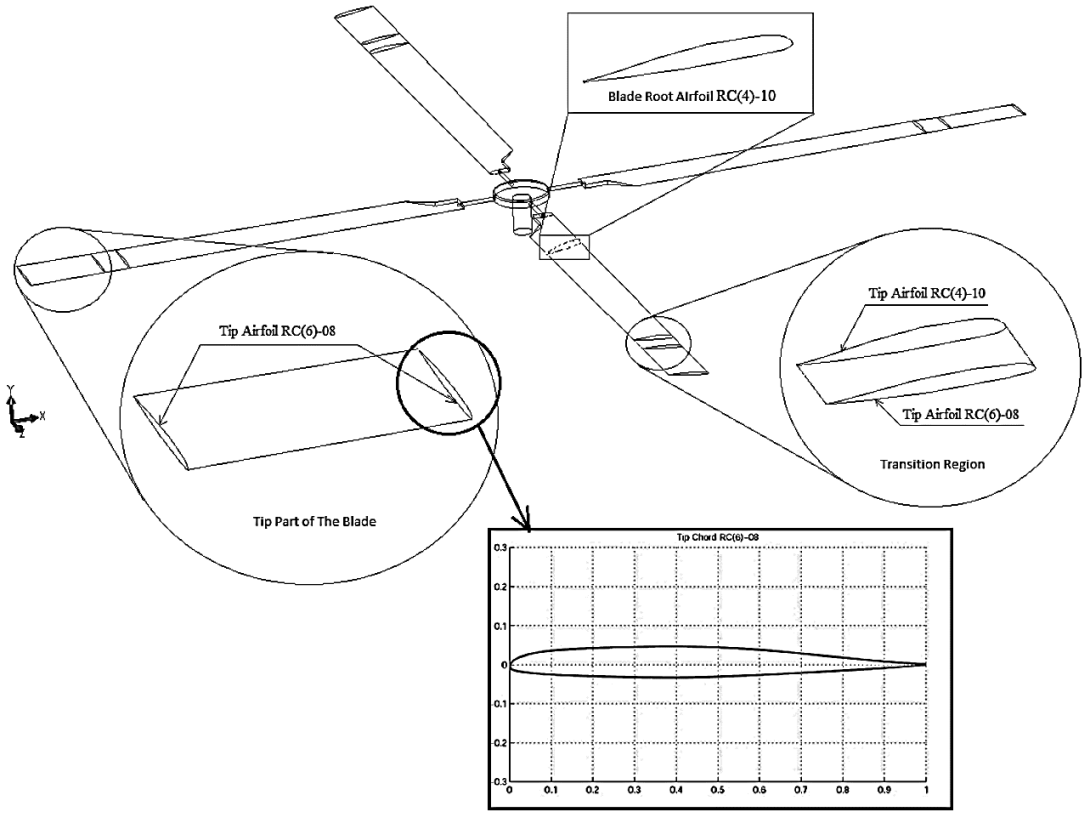

Figure 6. Tip chord profile [5].

6.2. Software Validation and mesh Comparison

Two types of mesh were used in this study to compare the structure and unstructured meshing strategies with three turbulence models SST-model, K-ε model and spalart-allmaras. Structure mesh is shown in Figure 7 The other mesh is unstructured mesh with three zones containing the airfoil which triangle is used for this mesh, as in Figure 8 Grid sensitivity is done by an increasing number of elements in meshing design (sizing and refinement) and by adapting the mesh in the solver by enhancement of the gradient of the static pressure and y+. The first type of mesh (structure) mesh reached approximately 300k elements with no change in the results. On the other hand, the second mesh (unstructured) mesh reached approximately 500k elements. For this airfoil the test tunnel data is available [6] and used to validate the simulated cases as shown in Figure 9 and Figure 10. Steady ideal gas condition with density based to suite high-speed compressible flow. The pressure far-field boundary is used to model free-stream condition at the domain end. The Coupled implicit formulation applied for more stable solution.

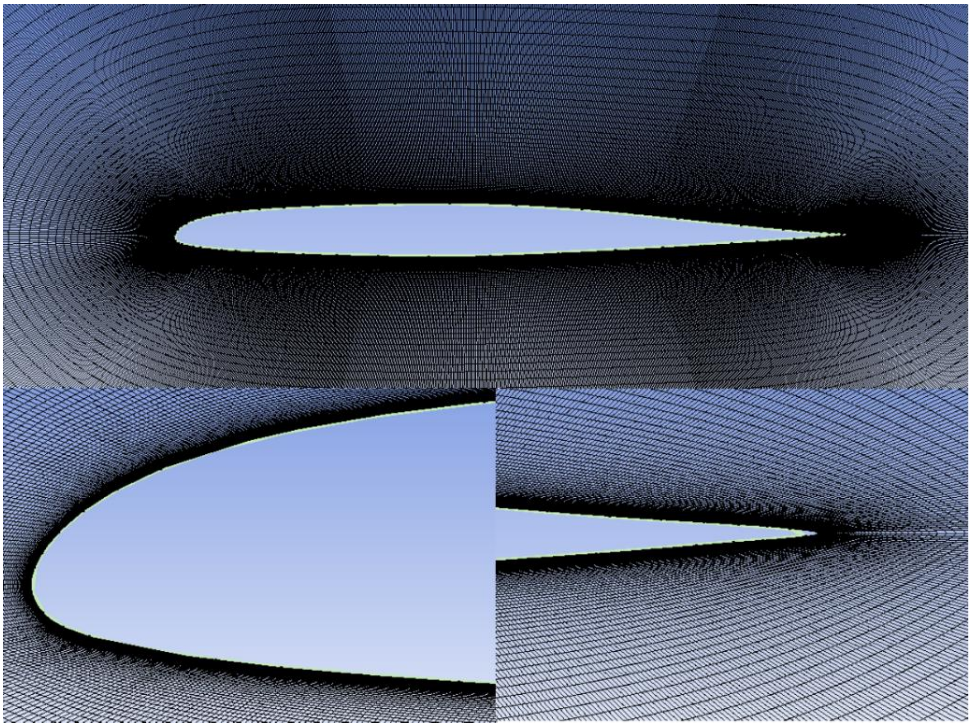

Figure 7. Structured mesh.

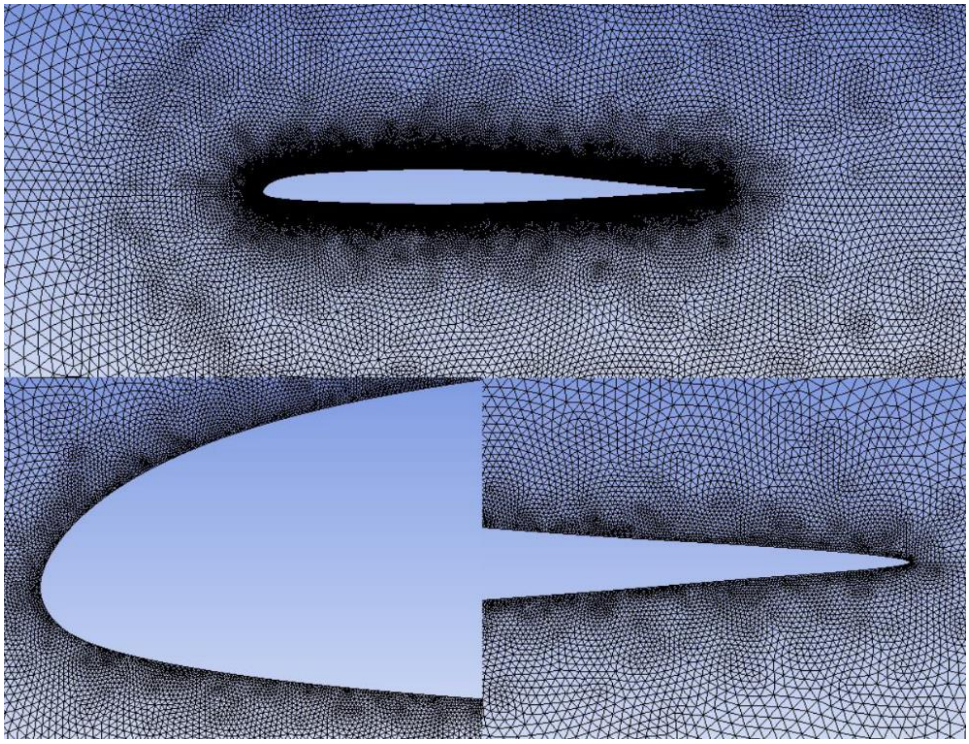

Figure 8. Unstructured mesh.

Because time steps converge faster and require fewer iterations, the SST-model (Shear Stress Transport Model) takes less than half the time of the K-Epsilon model. After increasing the angle of attack, the K-Epsilon model did not provide the same accurate value as when it was set at a low value. The SST-model gives suitable agreement for all simulated angles of attack. And the structured mesh also gives better agreement than the unstructured mesh. As conclusion, the SST-model has a mean error of 5% for lift coefficient and approximately 6% in drag coefficient using the structured mesh, which is the more accepted deviation than experimental data. This model will be chosen using structured mesh for further solution.

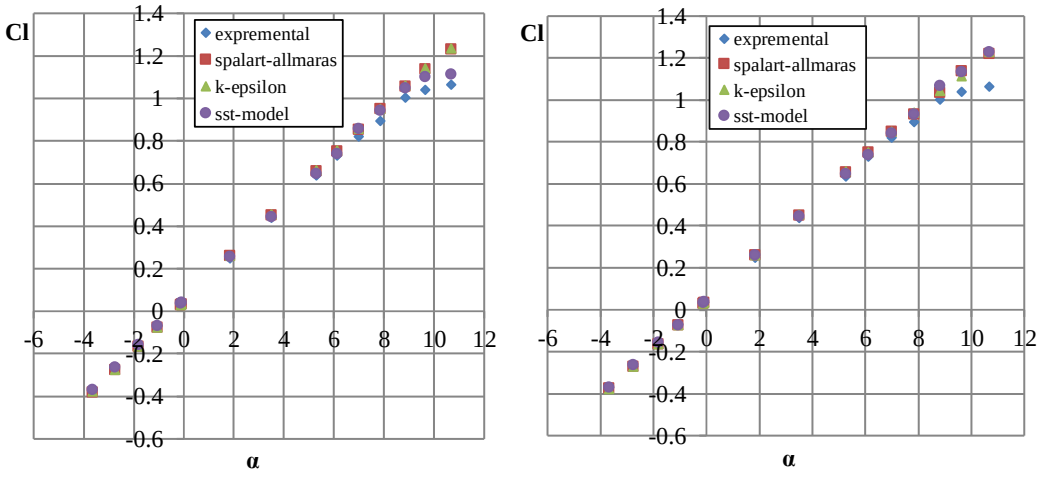

(a) (b)

Figure 9. Cl for used meshes (a) is structured and (b) is unstructured.

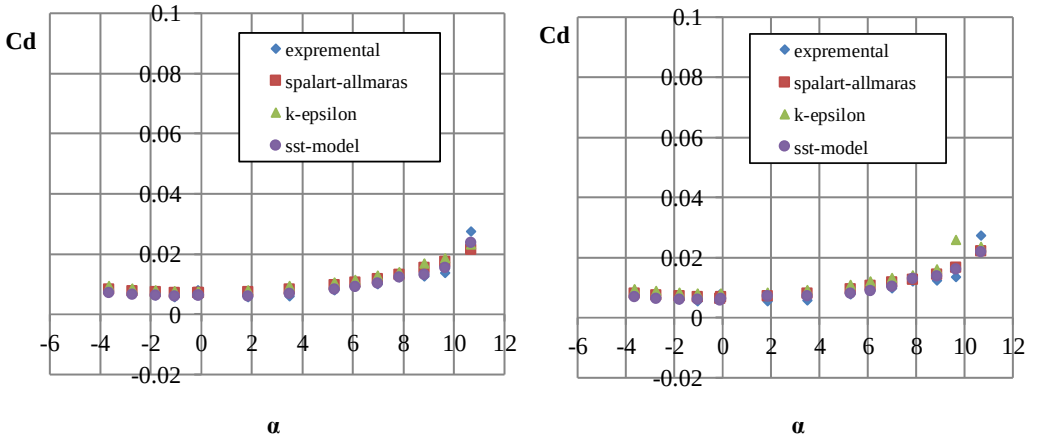

(a) (b)

Figure 10. Cd for used meshes (a) is structured and (b) is unstructured.

6.3. Controlled Cases

NASA published data as in [6] for the cross-section used in tip of the blade used in helicopter as shown in Figure 11. This data was selected where airfoil geometry existed, data is provided to be the base line case of this study "benchmark" and after that controlled cases can be solved based on the change over the benchmark case. 2-D simulation of the retreating side of the helicopter blade at the condition of forward speed. The advance ratio is selected as μ= 0.45 and μ= 0.15 where "Rotor advance ratio is the free stream velocity V_∞ with respect to rotor tip velocity". The value of the free stream Mach number will be M_∞= 0.28 and M_∞= 0.1 respectively. To correct for the pitch and roll moment, cyclic motion must be applied which increases the angle of attack at the retreating side, which can reach 10^o as a combination of collective and cyclic input at the tip of the blade [7][8][9] The relative Mach number at tip is the subtraction of the tip motion and free stream motion which results in low speed in the retreating side M_r=0.347 and M_r=0.527 respectively.

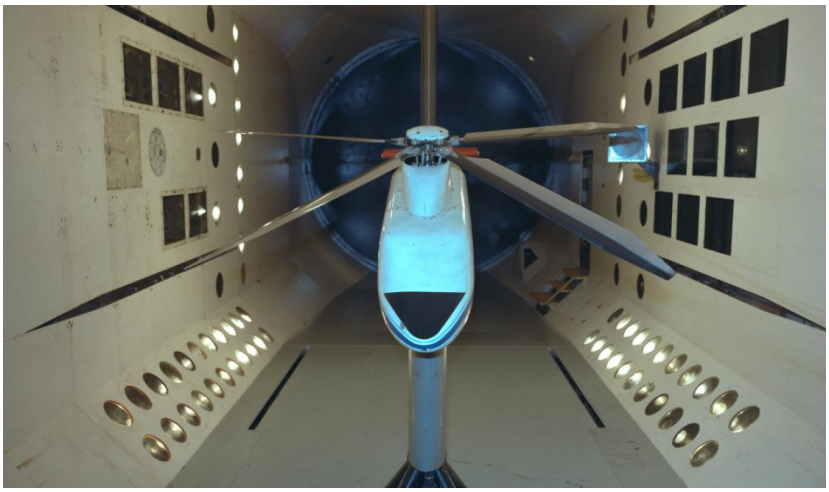

Figure 11. ARES test bed in Langley Transonic Dynamics Tunnel reported by NASA [6].

6.4. Control Parameters Selection

In Table 1 the summarized control parameter definition and values which are used in active flow control as shown in Figure 12:

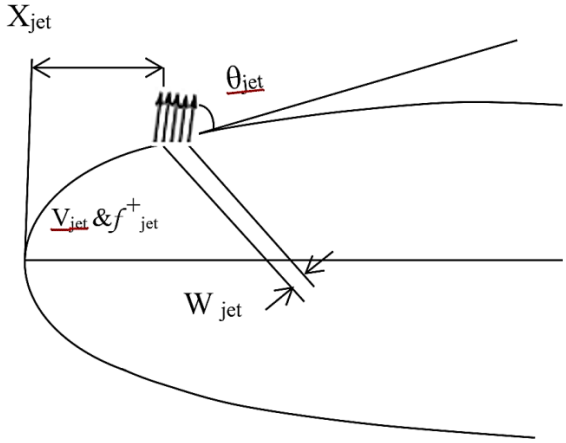

Figure 12. Simulation parameters.

Table 1. Control parameter.

Parameter definition	Jet width	Jet position	Jet Angle	Jet velocity	Jet frequency
symbol	$W^+= W_{Jet}/c$	$X^+= X_{Jet}/c$	θ_{jet}	$V_{Jet}(t) = \lVert V_o \sin(2\pi f^+ (V_\infty/c)\, t) \rVert$	$f^+= f_{Jet}/f_n$
Based studies	[10]	[11][12]	[13][14][15]	[16][17]	[16][17]
values	1.5%	0.055, 0.074, 0.09, 0.2	10°	V_o= 0.1, 0.01 V_∞	0.1, 1, 10

7. Results and discussion

Forward flight cases are simulated at different excitation parameters to study the effect of flow control on the airfoil used in helicopter blade as shown in Table 2. Two different forward flight conditions are simulated at different advance ratio of μ= 0.45 and μ= 0.15.

Table 2. Forward flight cases identification with selected parameter of each case.

μ	μ =0.45						μ =0.15					
v_{jet}	v_{jet} =0.1			v_{jet} =0.01			v_{jet} =0.1			v_{jet} =0.01		
f^+	f^+=0.1	f^+=1	f^+=10	f^+=0.1	f^+=1	f^+=10	f^+=0.1	f^+=1	f^+=10	f^+=0.1	f^+=1	f^+=10
X^+= 0.055	Case 49	Case 50	Case 51	Case 52	Case 53	Case 54	Case 73	Case 74	Case 75	Case 76	Case 77	Case 78
X^+= 0.074	Case 55	Case 56	Case 57	Case 58	Case 59	Case 60	Case 79	Case 80	Case 81	Case 82	Case 83	Case 84
X^+= 0.09	Case 61	Case 62	Case 63	Case 64	Case 65	Case 66	Case 85	Case 86	Case 87	Case 88	Case 89	Case 90
X^+= 0.2	Case 67	Case 68	Case 69	Case 70	Case 71	Case 72	Case 91	Case 92	Case 93	Case 94	Case 95	Case 96

Summarized results for performance parameters are presented in the next figures where all results for μ=0.45 are mentioned in **Figure 13** and results for μ= 0.15 are presented in Figure 14, which (a) represent the jet velocity V_{jet} =0.1V_∞ and (b) represent the jet velocity V_{jet} =0.01$V\infty$ the percentage change of the lift coefficient, drag coefficient and total performance represented by lift to drag ratio is plotted with different excitation location and frequency. As founded before in the results published in hover case of flight [18] the best performance enhancement was for the excitation location of X^+=0.2, which is a good indication for possibilities of applying this type of control in all modes of flight, which gives enhancement in every mode, and this can address the idea of continuous control using any blowing source for example small actuated cavity or bleed air. Furthermore, it can give more enhancement in

more forward speed as shown in μ= 0.45 results as expected because of the effect of retreating side where separation is increased.

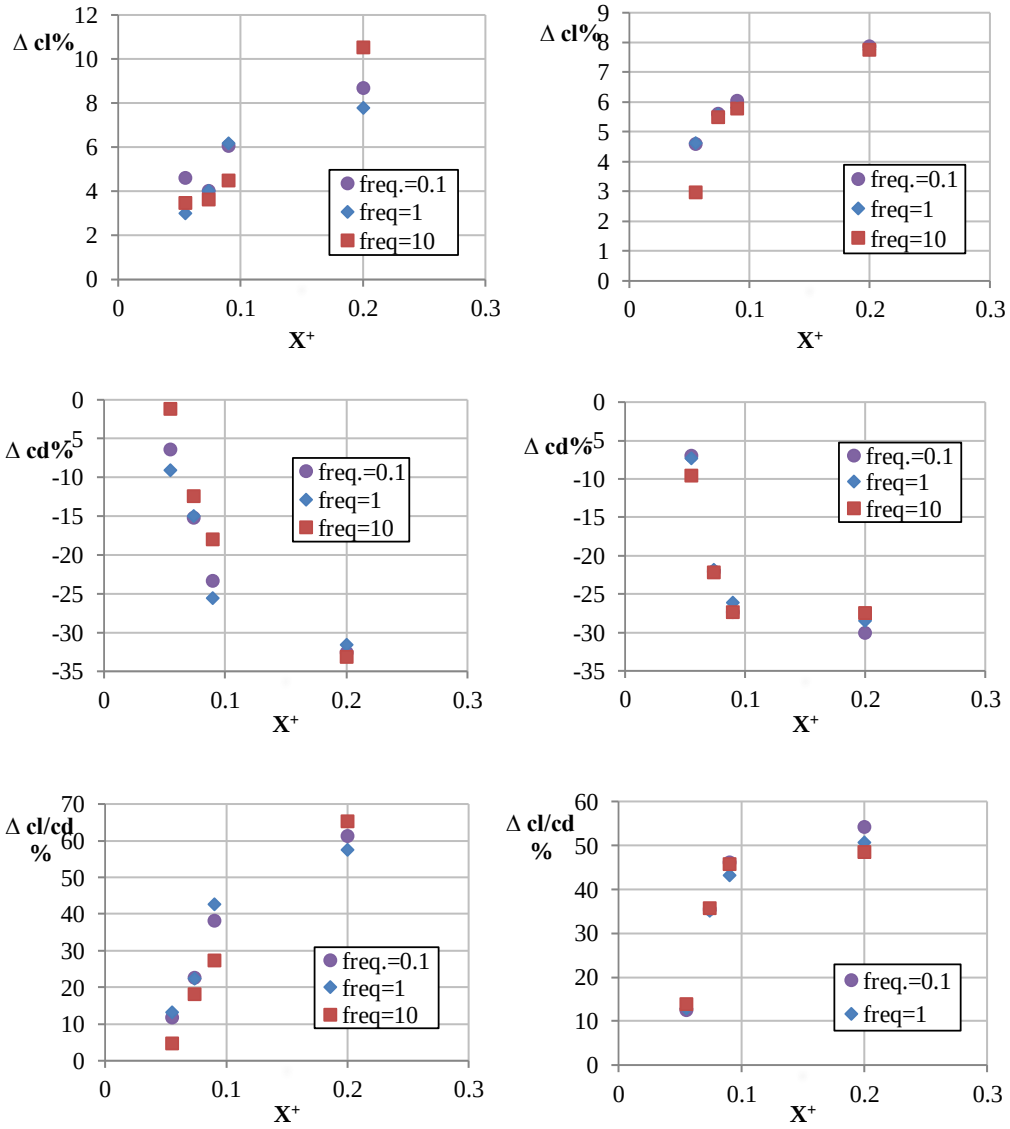

(a) V_{jet} =0.1V_{∞} *(b) V_{jet} =0.01V_{∞}.*

Figure 13. Results of harmonic jet test at μ =0.45 for the forward flight case study with angle of attack 10°.

.

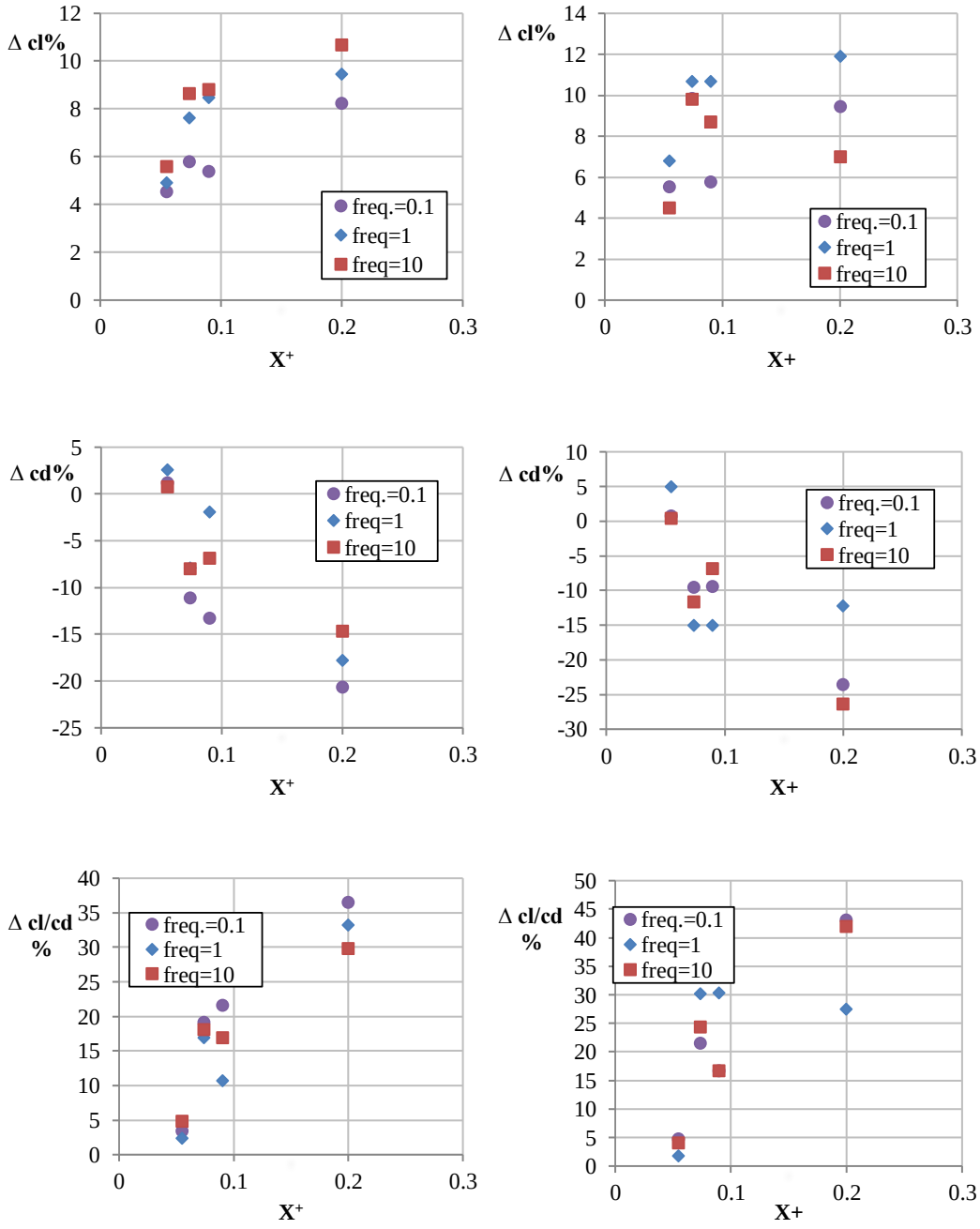

(a) V_{jet} =0.1V_∞ *(b) V_{jet} =0.01V_∞.*

Figure 14. Results of harmonic jet test at μ = 0.15 for the forward flight case study with angle of attack 10°.

The presenter results show the effect of the applied control on the forward flight state with $\mu = 0.15$ which helps the flow to reattach over the upper surface of the airfoil where the pressure is regained again and total performance is enhanced due to this separation recovery.

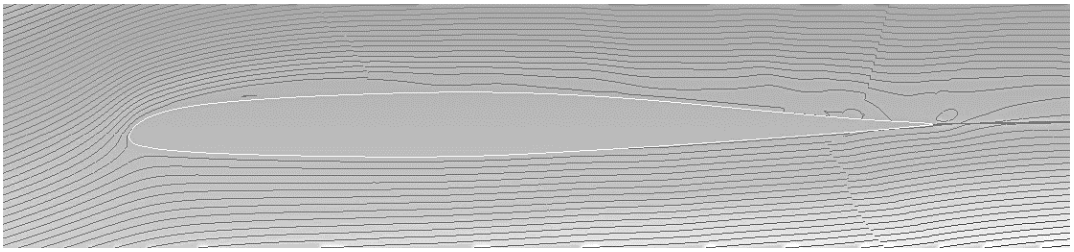

(a) Benchmark case

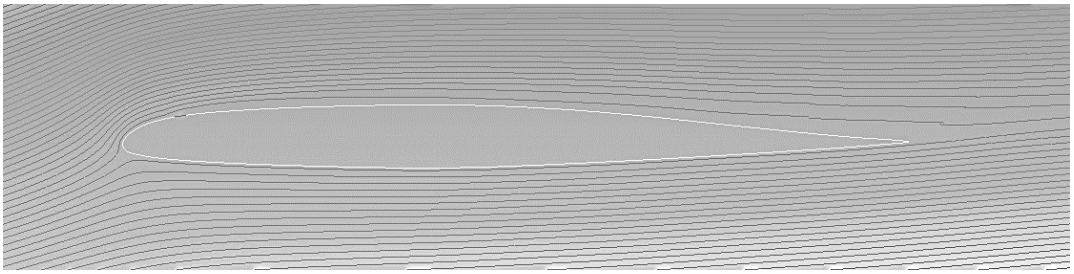

(b) Controlled case

Figure 15. Stream function distribution for selected case study compared with benchmark case at $X^{+}=0.2$, $f^{+}=1$ and $V_{jet}=0.1V_{\infty}$.

As shown in Figure 15 and Figure 16, the effect of this control on the airfoil used in blade in forward flight state at $\mu = 0.15$, case was selected at the most effective excitation position $X^{+}=0.2$, $f^{+}=1$, $V_{jet}=0.1V_{\infty}$ and at collective pitch $\theta_0=10^{o}$ which helps the flow on the blade to reattach over the upper surface of the airfoil which the pressure is regained again and total performance is enhanced due to this recovery. the main idea of flow control that works in the boundary region to increase the turbulence of the flow on a very small scale, that gives the flow the ability to flow near the wall again, which has the main impact of the pressure on the upper surface of the airfoil and as known the lift produced is a sum of the total pressure distribution along the airfoil and due to the separation a large part of the airfoil is not subjected to a flow of air as shown in the benchmark case which at this angle of attack "10^{o}".

More than 60% of the upper surface is covered by separation due to the required balance needed for a helicopter to balance the rolling effect produced by the dissymmetry of lift coming from the natural of single rotor helicopter as mentioned before in the aerodynamic characteristic described before.

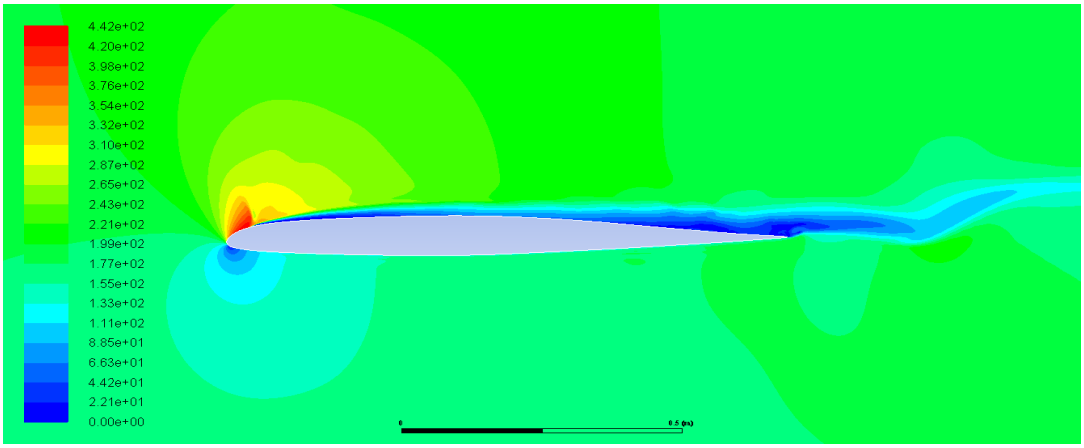

(a) Benchmark

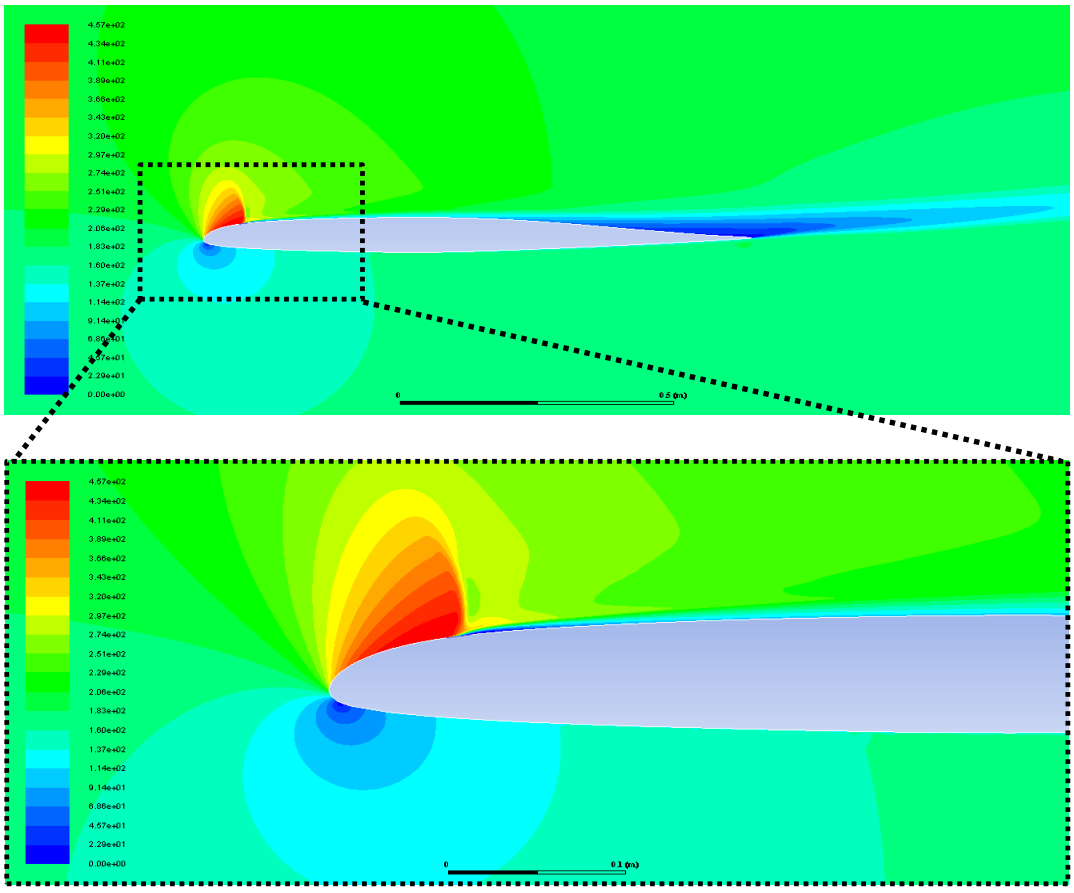

(b) Controlled case

Figure 16. Velocity contours shows that flow reattached due to control applied for selected case study compared with benchmark case at X^{+}=0.2, f^{+}=1 and V_{jet} =0.1V_{∞}.

8.Conclusion

As a part of a study to find the effect of the application of active flow control over a real tested helicopter hub blade, more than state of flight are tested and compared to the experimental results available. Hover state of flight has been previously published in where it was clear that in this mode of flight, active flow control can be used to enhance the hover performance of the helicopter. In this paper, another state of fight is simulated to find the ability to enhance the overall performance in forward flight conditions at different velocities represented in advance ratio μ. As expected, the results show more enhancement than the hover tested cases due to the retreating blade effect and relative velocity over the tip airfoil, which results shows 10% increase in lift and 30% decrease in drag which represents about 50% change in lift to drag ratio. This is not the only gain that this control can add, but also the idea of delaying the separation can solve a big problem that restricts the helicopter's forward speed due to what is called retreating blade stall. By enhancing the separation on retreating side, helicopter can go faster and velocity never exceed limit can be moves forward also vibration will be less in this condition due to less turbulence of the retreating blade. Enhancing the performance and vibration have a positive effect on the helicopter structure and fuel consumption, which leads to more economical operation of the helicopter. A 3D simulation will be tested in the next step of this study using complete main rotor hub that was used by NACA to see more accurate results using active flow control to improve the retreating blade stall.

References

[1] Prouty 2005, RW P Helicopter Performance of Stability and Control, *PWS Engineering Boston*.
[2] Caradonna, F X and Isom M P 1972, Subsonic and Transonic Potential Flow over Helicopter Rotor Blades, *AIAA Journal*, No. 12, pp. 1606-1612.
[3] Chang I C 1984, Transonic Flow Analysis for Rotors, *NASA TP* 2375.
[4] Xu M, Mamou M and Khalid M 2002, Numerical Investigation of Turbulent Flow Past a Four Bladed Helicopter Rotor Using k-ω SST Model, *The 10th Annual Conference of CFD Society of Canada*, Windsor.
[5] Kevin W Noonan, William T Yeager Jr, Jerey D Singelton, Matthew L, Wilbur and Paul H Mirick 2001, Wind Tunnel Evaluation of a Model Helicopter Main-Rotor Blade with Slotted Airfoils at the Tip, *NASA TP*-2001-211260.
[6] Kevin W Noonan MAY 1991, Aerodynamic Characteristics of a Rotorcraft Airfoil Designed for the Tip Region of a Main Rotor Blade, *Technical Report 91* -B-003.
[7] M F Yaakub, A A Wahab, A Abdullah, N A R Nik Mohd and S S Shamsuddin June 2017, Aerodynamic prediction of helicopter rotor in forward flight using blade element theory, *Journal of Mechanical Engineering and Sciences*.
[8] L I Garipova, A N Kusyumov, G Barakos, A N Tupolev 2014, CFD modeling of 2nd aerofoil dynamic stall, *29th congress of the international council of the aeronautical sciences*.
[9] Wieńczysław Stalewski 2018, Flow Control on Helicopter-Rotor Blades Via Active Gurney Flap, *Transactions of The Institute of Aviation*.
[10] R E and J A Weiberg 1952, Dannenberg, Section Characteristics of a 10.5-Percent-Thick Airfoil with Area Suction as Affected by Chordwise Distribution of Permeability, *DTIC Document*.
[11] Reni Raju, Rajat Mittal Louis and Cattafesta December 2008, Dynamics of Airfoil Separation Control Using Zero-Net Mass-Flux Forcing, *AIAA journal*, Vol. 46, No. 12.
[12] Arinin Ghoddoussi, Arinin Ghoddoussi July 2011, A Conceptual Study of Airfoil Performance Enhancements Using CFD, *Department of Aerospace Engineering and the faculty of the Graduate School of Wichita State University*.
[13] M Serdar GENÇ and Ünver KAYNAK May 2009, Control of Laminar Separation Bubble over a NACA2415 Airfoil at Low Re Transitional Flow Using Blowing/Suction, *13th International Conference on Aerospace Sciences & Aviation Technology*.
[14] L Huang, P G Huang, R P LeBeau and T Hauser February 2004, Numerical Study of Blowing and Suction Control Mechanism on NACA0012 Airfoil, *AIAA JOURNAL OF AIRCRAFT*.
[15] M Goodarzi, M Rahimi, R Fereidouni 2012, Investigation of Active Flow Control over

NACA0015 Airfoil Via Blowing, Mechanical Engineering Department, Engineering Faculty of Bu-Ali Sina University, Hamadan, Iran, *International Journal of Aerospace Sciences*.

[16] Bar Sever 1989, Separation Control on an Airfoil by Periodic Forcing, *AIAA Journal*, Vol. 27, No. 6.

[17] Wygnanski I 2000, Some New Observations Affecting the Control of Separation by Periodic Forcing, *AIAA Paper 2000*-2314.

[18] Tarek Mokhtar Tawfik Soltan, M M Abdelrahman and Y k Hassan 2022, Helicopter performance enhancement at hover state of flight by Appling active flow control over special tip airfoil, *international conference on applied mechanics and mechanical engineering*.

[19] Fotios K Tsiachris June 2005, Retreating Blade Stall Control on A NACA 0015 Aerofoil By Means of a Trailing Edge Flap, *Thesis submitted to the Faculty of Engineering*, University of Glasgow.

[20] Alex Zanotti 2012, Retreating Blade Dynamic Stall, *Doctoral Programme in Rotary Wing Aircrafts*.

[21] Patrick Bowles, Thomas Corkey and Eric Matlis January 2009, Stall detection on a leading-edge plasma actuated pitching airfoil utilizing onboard measurement, *47th AIAA Aerospace Sciences Meeting and Exhibit*, Orlando.

[22] Yashwanth Ram Ganti 2012, CFD Analysis of a Slatted UH-60 Rotor in Hover, *Thesis submitted to the Faculty of the Graduate School of the University of Maryland*.

[23] Wienczyslaw S and J Sznajder 2014, Computational Investigations of Active Flow Control on Helicopter-Rotor Blades, *Journal of KONES Powertrain and Transport*.